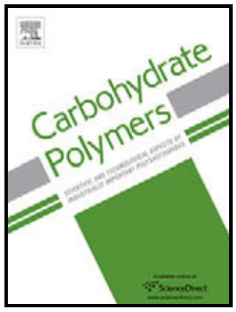

Title: CHITOSAN NANOPARTICLES FOR COMBINED DRUG DELIVERY AND MAGNETIC HYPERTHERMIA: FROM PREPARATION TO IN VITRO STUDIES

Author: Vanessa Zamora-Mora Mar Fernández-Gutiérrez Álvaro González-Gómez Beatriz Sanz Julio San Román Gerardo F. Goya Rebeca Hernández Carmen Mijangos

PII: S0144-8617(16)31149-3
DOI: http://dx.doi.org/doi:10.1016/j.carbpol.2016.09.084
Reference: CARP 11611

To appear in:

Received date: 29-1-2016
Revised date: 21-9-2016
Accepted date: 27-9-2016

Please cite this article as: Zamora-Mora, Vanessa., Fernández-Gutiérrez, Mar., González-Gómez, Álvaro., Sanz, Beatriz., Román, Julio San., Goya, Gerardo F., Hernández, Rebeca., & Mijangos, Carmen., CHITOSAN NANOPARTICLES FOR COMBINED DRUG DELIVERY AND MAGNETIC HYPERTHERMIA: FROM PREPARATION TO IN VITRO STUDIES.*Carbohydrate Polymers* http://dx.doi.org/10.1016/j.carbpol.2016.09.084

CHITOSAN NANOPARTICLES FOR COMBINED DRUG DELIVERY AND MAGNETIC HYPERTHERMIA: FROM PREPARATION TO IN VITRO STUDIES

Vanessa Zamora-Mora[1], Mar Fernández-Gutiérrez[1,2], Álvaro González-Gómez[1,2], Beatriz Sanz[3,4], Julio San Román[1,2], Gerardo F. Goya[3,4], Rebeca Hernández[1*], Carmen Mijangos[1]

[1] Instituto de Ciencia y Tecnología de Polímeros (CSIC), c/ Juan de la Cierva, 3, 28006 MADRID, Spain

[2] CIBER-BBN, c/ Monforte de Lemos 3-5, Pabellón 11, 28029, Madrid, Spain

[3] Nanoscience Institute of Aragón, University of Zaragoza, Mariano Esquillor s/n, 50018, Zaragoza, Spain

[4] Department of Condensed Matter Physics, University of Zaragoza, Pedro Cerbuna 12, 50009, Zaragoza, Spain.

*To whom correspondence should be addressed: rhernandez@ictp.csic.es;

HIGHLIGHTS

- Chitosan nanoparticles (CSNPs) were prepared through crosslinking with tripolyphosphate salts
- Magnetic nanoparticles and 5-fluorouracyl (5-FU) were encapsulated within CSNPs
- 5-FU release measured after 30 days decreases with magnetic nanoparticles content
- CSNPs were successfully internalized over fibroblasts and A-172 cancer cells
- CSNPs induced cell apoptosis by combination of magnetic hyperthermia and chemotherapy

ABSTRACT

Chitosan nanoparticles (CSNPs) ionically crosslinked with tripolyphosphate salts (TPP) were employed as nanocarriers in combined drug delivery and magnetic hyperthermia (MH) therapy. To that aim, three different ferrofluid concentrations and a constant 5-fluorouracil (5-FU) concentration were efficiently encapsulated to yield magnetic CSNPs with core-shell morphology. *In vitro* experiments using normal cells, fibroblasts (FHB) and cancer cells, human glioblastoma A-172, showed that CSNPs presented a dose-dependent cytotoxicity and that they were successfully uptaken into both cell lines. The application of a MH treatment in A-172 cells resulted in a cell viability of 67-75% whereas no significant reduction of cell viability was observed for FHB. However, the A-172 cells showed re-growth populations 4 hours after the application of the MH treatment when CSNPs were loaded only with ferrofluid. Finally, a combined effect of MH and 5-FU release was observed with the application of a second MH treatment for CSNPs exhibiting a lower amount of released 5-FU. This result demonstrates the potential of CSNPs for the improvement of MH therapies.

KEYWORDS: chitosan, magnetic nanoparticles, drug delivery, cytotoxicity, uptake, magnetic hyperthermia, cancer cells, *in vitro* studies

1. Introduction

Chitosan (CS) is a natural polymer obtained from extensive deacetylation of chitin, the second most abundant polysaccharide on earth after cellulose. It is mainly composed of two kinds of structural units: 2-amino-2-deoxy-d-glucose and *N*-acetyl-2-amino-2-deoxy-d-glucose linked by a β(1 → 4) bond. Chemical modification via its amino or primary and secondary hydroxyl groups results in molecular structures with additional functionalities (C. Peniche, F.M. Goycoolea & Argüelles-Monal, 2008 ; Fernández-Quiroz et al., 2015). Chitosan is inherently biodegradable and biocompatible and it has attracted a lot of attention over the last few years for the development of biomedical applications. (Dash, Chiellini, Ottenbrite & Chiellini, 2011; de la Fuente, Raviña, Paolicelli, Sanchez, Seijo & Alonso, 2010; Muzzarelli & Muzzarelli, 2005). Among them, chitosan nanoparticles provide interesting opportunities as nanocarriers of antitumoral drugs employed for chemotherapy (Chen et al., 2014; Deng, Zhen, Hu, Wu, Xu & Chu, 2011; Lozano, Torrecilla, Torres, Vidal, Domínguez & Alonso, 2008; Unsoy, Khodadust, Yalcin, Mutlu & Gunduz, 2014). Chemotherapy can be combined with other cancer treatments in order to induce a higher efficacy in the treatment by producing a synergistic therapeutic effect and improving tumor regression(Hervault & Thanh, 2014; Kumar & Mohammad, 2011; Mignani, Bryszewska, Klajnert-Maculewicz, Zablocka & Majoral, 2015). In this sense, some studies employing chitosan as main polymer have been reported, as an example, polymer nanoparticles prepared from partially quaternized derivatives of chitosan have been employed for combined cancer treatments based on gene therapy and drug release of paclitaxel. These nanoparticles were capable of improving the intestinal absorption, enhance cellular uptake, and avoid lysosomal entrapment (Wei et al., 2013)

Hyperthermia is another clinical therapy used concurrently with chemotherapy to achieve a synergistic effect for the combined treatment(Huang, Neoh, Xu, Kang & Chiong, 2012). The basis of the hyperthermia protocol is to increase the temperature of target cells to 41-46 $^{\circ}$C to impair the cell's repair mechanisms.(Jordan, Scholz, Wust, Fähling & Roland, 1999; Laurent, Dutz, Häfeli & Mahmoudi, 2011) Recently, the use of magnetic nanoparticles (mainly magnetite, Fe_3O_4) as heating agents has been approved for clinical uses, originating a new therapy called magnetic hyperthermia (MH). The heating during MH is based on the energy absorbed by the magnetic nanoparticles under irradiation with a low-frequency (*i.e.*, 100 kHz – 900 kHz) alternating magnetic field (AMF). The particles transform the energy of the magnetic field into heat by different physical mechanisms, and the transformation efficiency strongly depends on the nature of the particles such as particle size (Goya et al., 2008), agglomeration state (Gupta & Gupta, 2005) and viscosity of the surrounding medium. On the other hand, the application of a AMF to polymer drug carriers containing magnetic nanoparticles may accelerate the drug release rate as recently demonstrated for carboxymethyl chitosan and carrageenan beads (Mahdavinia, Etemadi & Soleymani, 2015) or carboxymethyl dextran -coated magnetoliposomes (Guo, Chen, Sun, Liu, Li & Wang, 2015). This result has been attributed to the motion of the MNPs originated by the application of the AMF that leads to the relaxation of the polymer chains.

There are few studies about CSNPs loaded with magnetic nanoparticles for hyperthermia applications. As example, Fe_3O_4-chitosan magnetic nanoparticles were obtained via suspension crosslinking method employing glutaraldehyde as the crosslinker and iron oxide nanoparticles obtained by coprecipitation. The application of an AMF gave rise to an increase of temperature measured in physiological saline suspensions (Zhao, Wang, Zeng, Xia & Tang, 2009). In another example, iron oxide

magnetic particles were coated with chitosan by spray-drying method. The application of an alternating magnetic field gave rise to a temperature increase of 7 °C (from 25 °C to 32 °C) (Donadel, Felisberto, Fávere, Rigoni, Batistela & Laranjeira, 2008). In a recent study, we demonstrated that the crosslinking reaction of chitosan with sodium tripolyphosphate (TPP) constitutes a mild and efficient method to encapsulate magnetic iron oxide nanoparticles (MNPs) giving rise to magnetic CSNPs with a core-shell morphology. Very importantly, aqueous dispersions of magnetic CSNPs undergo an increase of temperature when subjected to an alternating magnetic field ((f=580 kHz, H=24kA/m)(Zamora-Mora, Fernández-Gutiérrez, Román, Goya, Hernández & Mijangos, 2014).

To the best of our knowledge, this is the first time that CSNPs are evaluated through *in vitro* studies for their application in a combined chemotherapy and magnetic hyperthermia therapy. To that aim, CSNPs were loaded with a model antitumoral drug, 5-fluorouracil (5-FU) and MNPs. The 5-FU release from CSNPs loaded with different amounts of MNPs was evaluated at physiological temperature and pH. CSNPs were tested for their cytotoxicity and their *in vitro* magnetic hyperthermia performance after being internalized in connective cells (fibroblasts) and malignant human glioblastoma cells (A-172). The results obtained from the combined therapy, magnetic hyperthermia and chemotherapy, were compared to those obtained for CSNPs loaded with MNPs or 5-FU separately in order to quantify the efficiency for each of the individual treatments.

2. Materials and methods

2.1. Materials

Chitosan employed in this work was isolated from shrimp's shell (*Heterocarpus vicarious*) and supplied by Polymers Laboratory, National University, Costa Rica. The degree of *N*-acetylation (DA= 0.12) chitosan was determined by ^{1}H-NMR (Figure S1) according to the procedure described by (Vårum, Antohonsen, Grasdalen & Smidsrød, 1991). The molecular weight of 362 KDa was determined by the viscosity method (ASTM D 2857). Oleic-acid-coated magnetic iron oxide nanoparticles (MNPs) dispersed in water as ferrofluid (density =1.08 g/mL), were provided by Nanogap Subnmparticles, Spain. According to the manufacturer, the crystalline form of the iron oxide nanoparticles is magnetite, Fe_3O_4 and their average size is 18.55 ±2 nm. Milli-Q (18.3 MΩ) water was used in all experiments. The following chemicals were purchased from Sigma-Aldrich Company (St. Louis, MO, USA) and used as received: sodium tripolyphosphate (TPP), 5-Fluorouracil (5-FU) and phosphate buffered saline (PBS pH=7.4).

2.2. Preparation of 5-fluorouracil (5-FU) and magnetic nanoparticles loaded chitosan nanoparticles

A determined amount of pure ferrofluid was dispersed in 5 mL of milli-Q water to yield final ferrofluid concentrations of 5, 20 and 50 mg/mL. Each of these ferrofluid solutions were mixed under mechanical stirring in a N_2 atmosphere with a chitosan solution (0.5% w/v) in a volumetric ratio chitosan: ferrofluid of 6:1. Separately, 5-fluorouracil was dissolved in an aqueous solution of sodium tripolyphosphate (TPP) (0.5% w/v), to a final concentration of 0.5% (w/v). Then, 6 mL of the aqueous solution containing 5-FU and TPP was added dropwise into the aqueous solution containing

chitosan (30 mL) and ferrofluid (5 mL) under mechanical dispersion at 8600 rpm, followed by stirring for 10 min at room temperature. The 5-FU concentration was chosen based on the IC50 results obtained for 5-FU in FBH (24.06 mg/mL) and A-172 cells (4.04 mg/mL) (results shown in supplementary information, figure S2). A concentration below IC50 is needed in order to ensure activity of the drug at non cytotoxic concentrations for the cells. CSNPs were collected by centrifugation at 5000 rpm for 20 min. Finally, the supernatant was separated and then it was freeze-dried. 5-FU and ferrofluid loaded chitosan NPs were named 5-FU-CS-MNPx, where x correspond to the Fe_3O_4-MNPs concentration. The Fe_3O_4-MNPs concentration in the CSNPs was determined by measuring their Fe contents through UV-VIS transmission spectrophotometry (Shimadzu UV-160), based on the thiocyanate complexation reaction(Gupta & Gupta, 2005):

$$Fe^{3+}_{(aq)} + 6\,SCN^{-}_{(aq)} \rightarrow \lfloor Fe(SCN)_6 \rfloor^{3-}_{(aq)}$$

CSNPs were dissolved in HCl 6 M-HNO3 (65%) at 60 ^{0}C during 2 h. Potassium thiocyanate was then added to the Fe^{3+} solution to form the iron-thiocyanate complex, which has strong absorbance at 478 nm wavelength. The iron concentration was determined by comparing the sample absorbance to a calibration curve. For each of the initial concentrations of ferrofluid employed in the preparation of CSNPs (5, 20 and 50 mg/mL), the final MNPs concentration achieved was 1, 3.2 and 5.6 mg/mL.

As a control material, chitosan NPs loaded only with MNPs were prepared following a method reported elsewhere (Zamora-Mora, Fernández-Gutiérrez, Román, Goya, Hernández & Mijangos, 2014). Sample was denoted as CS-MNP5.6 where the number refers to the iron concentration determined by UV-vis spectroscopy. A second control sample was prepared by encapsulation of only 5-FU and named 5-FU-CS-NPs.

5-FU-CS-NPs were obtained by dropwise addition of an aqueous solution containing TPP and 5-FU into a chitosan stock solution (0.5% w/v) in a ratio chitosan: TPP+5-FU of 5:1, under mechanical stirring (8600 rpm) at room temperature. The resulting aqueous dispersion of 5-FU-CS-NPs was centrifuged at 5000 rpm during 20 min (centrifuge Sigma 2-16P). The precipitate was discarded and the supernatant fraction was subjected to freeze-drying.

2.3. Physicochemical and morphological characterization

Micrographs of the samples were taken using a field emission scanning electron microscope (FESEM) Hitachi model SU8000 HRSEM (Hitachi High-Technologies Corporation, Tokyo, Japan) used in the TE (electron transmission) detector bright field mode. For visualization of CSNPs by FESEM, one drop of aqueous dispersions of the samples was deposited on the Formvar-carbon-coated Cu grid.

Dynamic Light Scattering (DLS) was used for the determination of the CSNPs hydrodynamic diameter and ζ–potential employing a Malvern Nanosizer Nazo ZS (Malvern Instruments Ltd, United Kingdom) with a 633 nm laser diode and a backscattering detection angle of 173º. Samples were dispersed in milli-Q water at 25 °C and the resulting pH of the dispersions was 4.5. The electrophoretic mobility was transformed into ζ–potential employing the Smoluchowski equation. All measurements were repeated three times and the average of three runs was taken as the result.

Attenuated Total Reflection Fourier Transformed Infrared Spectroscopy (ATR-FTIR) was carried out on freeze-dried samples. Spectra were measured in a Spectrum One FT-IR Spectrometer of Perkin Elmer (PerkinElmer Life and Analytical Sciences, USA) in the wave number range of 650-4000 cm^{-1} and with 4 cm^{-1} resolution.

2.4. Evaluation of drug encapsulation efficiency and loading efficiency.

For the determination of encapsulation efficiency (EE) of 5-FU within CSNPs, samples were centrifuged at 12000 rpm for 30 min, using centrifuge tubes IVSS Vivaspin 20, with a pore size of 3000 MWCO, to recover the residual fraction containing the 5-FU free. Then, this fraction was measured by ultraviolet spectroscopy (Perkin Elmer Instrument Lambda 35 UV/VIS spectrometer). 5-FU was measured at 265 nm where an intense characteristic peak was displayed. The encapsulation efficiency was calculated according to the following equation (Papadimitriou, Bikiaris, Avgoustakis, Karavas & Georgarakis, 2008):

$$EE = \left(\frac{(Total\ amount\ of\ 5{-}FU) - (amount\ of\ free\ 5{-}FU)}{Total\ amount\ of\ 5{-}FU}\right) x\ 100 \qquad \textit{Equation 1}$$

The loading efficiency of 5-FU loaded into 5-FU-CS-NPs and 5-FU-CS-MNPs samples was determined from the freeze-dried samples as follows: a known weight of freeze-dried samples was dissolved in acetic acid (1% v/v). Then the drug content was analyzed using UV/Vis spectroscopy at 265 nm with the appropriate dilutions. The loading efficiency (LE) was calculated as follows:

$$LE = \left(\frac{(amount\ of\ 5{-}FU\ incorporated\ into\ nanoparticles)}{weight\ of\ freeze{-}dried\ sample}\right) x\ 100 \qquad \textit{Equation 2}$$

All measurements were performed in triplicate and the mean value calculated.

2.5. Evaluation of in vitro drug release.

The release of 5-FU from CSNPs was studied at physiological pH, according to the protocol of Zhu and coworkers (Zhu, Ma, Jia, Zhao & Shen, 2009) with some modifications. Each of the samples under study was dispersed to a concentration of 0.01% (w/v) in phosphate buffer solution (pH=7.4). Then, 3 mL of each dispersion was placed into a dialysis tubing (MWCO 3500-5000 Da) that was immersed in 10 mL of the buffer at 37 ºC with moderate orbital stirring. An aliquot of 1 mL was withdrawn

from the release medium at regular times and replaced with equivalent aliquots of fresh medium during 30 days. The kinetics of release of 5-FU from 5-FU-CS-NPs and 5-FU-CS-MNPs was measured by UV/Vis spectroscopy (Perkin Elmer Instrument Lambda 35 UV/VIS spectrometer, at 265 nm). All data reported are an average of three measurements.

2.6. Cytotoxicity study by Alamar Blue assay

The cytotoxicity of the 5-FU-CS-NPs and three 5-FU-CS-MNPs was measured through Alamar Blue (Mignani, Bryszewska, Klajnert-Maculewicz, Zablocka & Majoral) (provided by Serotec, Spain) assays for two cell lines, human dermal fibroblast (FBH-INNOPROT SPAIN) and malignant human glioblastoma cells (A-172-ECACC, UK). Samples were sterilized with a UV lamp (HNS OSRAM, 263 nm, 3.6UVC/W) at a power of 11 W for 2 h. Both cell lines were seeded into 96 wells plates at a density of 1 × 10^5 cells/mL (1 × 10^4 cells/well) in complete medium and incubated to confluence. After being cultured for 24 h, FBH and A-172 cells were treated with different aqueous dispersions of 5-FU-CS-NPs and 5-FU-CS-MNPs and incubated at 37 ºC in humidified air (95%) with 5% CO_2 for 24 h. After that, a solution of AB (10% v/v) prepared in a warm medium without phenol red was added to the plate and incubated at 37ºC for 4 h. Finally, fluorescence was measured with a Biotek Synergy HT detector using an emission wavelength of 590 nm and an excitation wavelength of 530 nm.

Cell viability (*CV*) was calculated with the following equation:

$$CV = 100 \times \left(\frac{FD_S - FD_B}{FD_C - FD_B}\right) \qquad \textit{Equation 3}$$

where FD_S, FD_B, and FD_C are the fluorescence density of the AB for the sample (S), blank (B) (culture medium without cells), and control (C), respectively.

2.7 Cellular uptake of chitosan nanoparticles

The cellular uptake of CSNPs was determined by epifluorescent microscopy, which is a method that allows observing the nanoparticles carrying a fluorescent label (sodium fluorescein dye 20%) in different cell lines (FBH and A-172). The experiment was as follows: a dispersion of fluorescent nanoparticles (0.06% (w/v) in medium without phenol red + fluorescein 0.01% v/v) was added to the cells seeded onto a glass dish in semi-confluence and incubated during 24 h at 37 ºC and 5% of CO_2. The cells were rinsed with phosphate buffered saline (PBS) and fixed with paraformaldehyde 3.7% in PBS for 10 min at 37 ºC. After that, paraformaldehyde was removed and cells were rinsed again with PBS. Finally, triton (Triton X-100, molecular biology grade, density 1.07 g/cm³) 0.05% (v/v) in PBS was added during 20 min at 37 ºC for permeability in the cellular membrane. The samples were rinsed with PBS and the cell nuclei were stained with 10 µL/mL of Hoechst H33342 dye solution. In addition, phalloidin (1 µL/ 100 µL) was used for staining the actin cytoskeleton of the cells and left it for 30 min at room temperature in the darkness. Finally, fluorescence was observed with an epifluorescence microscope (Nikon eclipse TE2000-S) and three different filters.

2.8. In vitro magnetic hyperthermia experiments

The magnetic hyperthermia experiments were performed using a commercial 10-kW induction heating system (EASYHEAT, Ambrell, UK) using a 9-turn coil of 5 cm diameter specifically designed to accommodate a 3.5 cm petri dish inside. The samples were thermally insulated from the coil by a water-refrigerated jacket. The alternating magnetic field (f = 180 kHz; H = 35 kA/m) was applied during 20 min to the cells in the petri dish, and after that the cell viability of the two cell lines (i.e., malignant human

glioblastoma (A-172) and fibroblast (FBH)) loaded with CSNPs was measured. A scheme of the experiment is shown in the supplementary information (Figure S3). Both cell lines (FBH and A-172) were seeded separately onto an Ibidi dish (µ-Dish 35 mm, sterile, low wall) at a density of 15×10^4 cells/mL in complete medium and incubated to confluence. After being cultured for 24 h, FBH and A-172 Ibidi dishes were treated with the corresponding dispersion of nanoparticles. Finally, after 24 h of incubation samples were exposed to the AC field during 20 min. After that, the samples were rinsed with PBS to remove dead cells and free CSNPs. Samples were fixed with glutaraldehyde 2.5% (v/v) at 37 °C after two different times, 10 min and 4 hours after the MH treatment (1MH). A second magnetic hyperthermia treatment (2 MH) was applied to A-172 cells and samples were fixed 4 h later. Crystal violet staining was used for determining cell viability. All the samples fixed, were treated with a 0.1% (w/v) of aqueous solution of crystal violet in PBS pH 7.2. After 10 min of incubation at room temperature under agitation, the staining solution was discarded; the samples were washed with Milli-Q water and then dried at 37 ºC. Finally, aqueous acetic acid (10% v/v) was added to the samples and an aliquot of 200 µL was taken and placed into a well of plates to determinate the relative viability by a microplate reader at 620 nm-690 nm.

All the samples after the cell fixation were treated with acridine orange and propidium iodide (AO/PI), to visualize living and dead cells simultaneously. Acridine orange (AO) is permeable to both live and dead cells and stains all nucleated cells to generate green fluorescence. On the other hand, propidium iodide (PI) enters dead cells with compromised membranes and stains all dead nucleated cells to generate red fluorescence. The procedure was as follows: all the samples fixed after magnetic hyperthermia treatment were rinsed with PBS and then triton (Triton X-100, molecular

biology grade, density 1.07 g/cm³) 0.05% (v/v) in PBS was added and the sample was maintained during 20 min at 37 ºC under low speed orbital shaking. After that, the samples were rinsed with PBS and 10 µL/mL of AO/PI staining solution was added and left it for 30 min at room temperature in the darkness. Finally, the samples were rinsed twice with Tween 20 solution at 0.1% in PBS and left it with Milli-Q water. Samples were observed in an epifluorescence microscope (Nikon eclipse TE2000-S) equipped with a FX-RED filter set to detect dead cells, and a FITC filter set to detect live cells.

3. **Results and discussion**

3.1 Physicochemical and morphological characterization

CSNPs loaded with 5-FU and MNP were successfully obtained by ionotropic coupling with TPP and it was corroborated by FESEM. The obtained nanoparticles are stable in the medium thanks to the ionotropic crosslinking of phosphate negative groups and free amine functions of the chitosan polymer chains(Fernandes, de Oliveira, Fatibello-Filho, Spinelli & Vieira, 2008; Yang et al., 2009). Figure 1 shows a representative FESEM image corresponding to sample 5-FU-CS-MNP3.2, in which it is possible to observe nanoparticles with particle size of 125±44 nm and a relatively high polydispersity which might be attributed to the method of preparation employed. Further information on the morphology obtained for the samples spread and dried on a glass surface can be obtained from atomic force microscopy images shown in figure S4.

The hydrodynamic diameter and ζ– potential of the CSNPs determined through DLS measurements is reported in table 1. As can be observed, the hydrodynamic diameter increases with the MNPs encapsulation from 183±2 nm in the sample 5-FU-CS-NPs to 255±9 nm in the sample 5-FU-CS-MNP5.6. Previous studies carried out on CSNPs loaded only with MNPs showed that the hydrodynamic diameter increased with the MNPs content. This was attributed to the fact that magnetite nanoparticles are subjected to Van der Waals forces and magnetic dipole-dipole interactions generated from residual magnetic moments that together may produce and increase in the particle size(Zamora-Mora, Fernández-Gutiérrez, Román, Goya, Hernández & Mijangos, 2014).

The ξ -potential, which is the electrostatic potential that exists at the shear plane of a particle, is related to both surface charge and the local environment of the particle (Rescignano et al., 2015). As previously reported, CSNPs crosslinked with TPP present a ξ-potential of +63.4±0.8 mV whereas commercial ferrofluid present a ζ–potential of -75.8±3.2 mV(Zamora-Mora, Fernández-Gutiérrez, Román, Goya, Hernández & Mijangos, 2014). As can be observed in table 1, the ξ-potential values found for CSNPs loaded with 5-FU and MNPs slightly decreases with respect to that found for CSNPs crosslinked with TPP (+63.4±0.8 nm) and remained positive in the range of +52-+59 Mv. This is abscribed to the protonated chitosan ammonium groups in the acidic environment that resulted from the dispersion of the CSNPs in milli-Q water and suggests the efficient encapsulation of the ferrofluid within the chitosan NPs. It is clear from these results that the ionotropic coupling allows the orientation of the more hydrophilic segments of the network structure, corresponding to sequences of glucosamine rings, forming a `shell´ structure of the nanoparticle which contributes to the high positive value of the ζ–potential. The MNPs interact with the polyphosphate-amine groups in the inner core of the CSNPs and remains in this position because of the network structure and morphology of the whole system.

Figure 2 shows the ATR-FTIR spectra corresponding to all the samples under study.

The presence of a strong band located at 1246 cm^{-1} which is attributed to C-F of 5-FU ring(Zhu, Ma, Jia, Zhao & Shen, 2009) in the spectra corresponding to CSNPs, confirms the encapsulation of 5-FU. The band located at 804 cm^{-1} in the spectra of 5-FU (figure 2a), attributed to C-H out of plane deformation of 5-FU ring, shifts to higher

wavenumbers in the samples containing 5-FU (figure 2b-d). These shifts suggest the presence of dipolar interactions between the polymer matrix and 5-FU. The spectrum corresponding to chitosan (figure 2-f) presents characteristic vibrational absorption bands located at 1652 cm^{-1} that corresponds to the amide I vibration (labelled as I in figure 2f) and at 1593 cm^{-1} corresponding to the N-H bending vibration overlapping the amide II vibration (labelled as II in figure 2f)(Lawrie et al., 2007). As can be observed, the position corresponding to band I in CSNPs containing 5-FU and MNPs does not change with respect to chitosan. In contrast, the band II located at 1597 cm^{-1} shifts to 1551 cm^{-1} in the ATR-FTIR spectrum corresponding to 5-FU-CS-NPs and to 1557 cm^{-1} in the ATR-FTIR spectrum corresponding to 5-FU-CS-MNP5.6. The larger shifts observed for samples loaded with MNPs suggest an additional interaction between them and 5-FU that will be corroborated by the results obtained from *in vitro* drug release experiments shown in the next section.

3.2 In vitro drug release

The encapsulation efficiency (EE) and loading efficiency (LE) of 5-FU within CSNPs was determined through UV-spectroscopy. All the samples presented very similar encapsulation efficiencies with values in the range 80-82%. These results agree with other investigations which report EE on the range of 80-85%(Wang, Zeng, Tu & Zhao, 2013). On the other hand, LE values obtained for all the samples are on the range 33-35%. According to the stoichiometry of the f**o**rmulation, theoretically a LE of 20% should be obtained. The experimental difference is attributed to the fact that the partial precipitation of chitosan nanoparticles during the process of washing after their preparation modifies the real total amount of the isolated dried sample and, according to equation 2, this yields a higher value of the LE with respect to the expected value.

The accumulative release profiles of the 5-FU chemotherapeutic agent measured at normal physiological pH and temperature are shown in **Figure 3**. After 30 days, the sample 5-FU-CS-NPs presents the highest % cumulative 5-FU release (45±4). Samples 5-FU-CS-MNP1 and 5-FU-CS-MNP3.2 present similar % cumulative 5-FU release after 30 days (30±3), however, for the sample with the highest content of MNPs 5-FU-CS-MNP5.6, the % cumulative 5-FU release sharply decreases to 15±1. This result can be attributed to the interaction established between 5-FU and the MNPs as determined through ATR-FTIR so that drug diffusion can be considered as controlled and modulated by the coupled system.

In addition, a close examination of the data plotted in figure 3 allows to observe that, for 5-FU-CS-MNP5.6, the % cumulative 5-FU release reaches a plateau after 2.5 days, whereas for the rest of the samples, it takes 4 days to attain a plateau in the % drug cumulative release. In this case, the establishment of stronger interactions between the MNPs and the 5-FU as a consequence of the higher amount of MNPs of the sample might be responsible for the lower cumulative drug release obtained and, at the same time, promote a more sustained release of 5-FU.

3.3 Cytotoxicity study

The cytotoxicity of all the samples under investigation was evaluated with the Alamar Blue assay. The experiments were tested in two cell lines, fibroblasts (FBH) and malignant human glioblastoma cells (A-172). Both cell lines were treated with CSNPs dispersed at different concentrations in medium without phenol red.

Figure 4 shows that both cell lines presented a dose-dependent effect on the cellular viability for all the nanoparticles under study. That is, the higher the concentration of nanoparticles in the aqueous dispersions, the lower the cell viability.

Specifically, CSNPs concentrations =5 mg/mL results in lower cell viability for normal cells, FBH with respect to cancer cells, A-172. This might be attributed to a higher resistance of cancer cells to the 5-FU treatment with respect to normal cells(Longley, Harkin & Johnston, 2003). This effect is also observed for FBH treated with 5-FU-CS-MNP5.6 (2.5 mg/mL) for which the cell viability decreases to 15% whereas for cancer cells, the cell viability is 60%. Based on these results, we selected a concentration of 0.6 mg/mL of chitosan nanoparticles for the rest of the biological experiments which proved to be non-cytotoxic for any of the cell lines.

3.4 Cellular uptake studies

The cellular uptakes of the CSNPs under study in FBH and A-172 cells after 24 h of incubation were measured through fluorescence technique using an epifluorescence microscope. Figure 5 shows fluorescence images corresponding to normal cells, FBH and cancer cells, A-172 incubated with sample 5-FU-CS-MNP5.6 for 24 h. To obtain a good observation of the fluorescence images, different dyes were used, 5-FU-CS-MNP5.6 were stained with sodium fluorescein dye (green), the cellular nuclei were stained using a Hoechst H33342 dye solution (blue) and the cytoskeleton of the cells were stained using phalloidin (Donadel, Felisberto, Fávere, Rigoni, Batistela & Laranjeira). The merged image (union of the three stains) shows that after 24 h of incubation, 5-FU-CS-MNP5.6 nanoparticles were successfully internalized into normal cells, FBH (inset figure 5) and cancer cells, A-172 as denoted by the presence of yellow

dots that corresponds to some agglomeration of CSNPs around the cellular nuclei for both cases. Similar results were obtained for the rest of the CSNPs under study (results not shown). Therefore, the results obtained show that the hydrodynamic diameter and ζ–potential of the three samples allows effective endocytosis into both cell lines.

3.5 In vitro magnetic hyperthermia

The effect of the applied magnetic field on the cell viability of FBH and A-172 cells was determined from crystal violet staining experiments carried out on cell lines treated with aqueous dispersions of sample 5-FU-CS-MNP5.6 at a concentration of 0.6 mg/mL (concentration determined from Alamar blue essays) and subjected to a single magnetic hyperthermia (1MH) treatment and two magnetic hyperthermia (2MH) treatments. The results obtained were compared to those corresponding to cells treated with chitosan NPs loaded with each of the therapeutic agents, 5-FU (5-FU-CS-NPs) and magnetic NPs (CS-MNP5.6) separately (Figure 6).

As can be observed, FBH and A-172 cells show cellular damage after 1 MH treatment as evidenced by the small spots that correspond to dead or apoptotic cells. Moreover, important changes of cell morphology such as cell shrinkage, densification of the cytoplasm and a tighter packing of cell organelles were noticed. These changes in the morphology suggest that cells undergo an apoptotic process (Elmore, 2007). Despite the low concentration of chitosan NPs used in these experiments, it is clear that it was possible to induce cell death through the application of an alternating magnetic field on chitosan NP-loaded cells. It is important to mention that no temperature increase was observed during the MH experiments, as measured by an infrared thermographic camera (see supplementary information, figure S5). This was expected from the low average concentration of magnetic NPs within the cell culture, and also the

geometry of the experiment (i.e., a single layer of adherent cells in a petri dish) that allows a fast heat exchange through the surface of the cell culture. The observed decrease in cell viability due to alternating magnetic field in MNP-loaded cells has been previously reported by many authors, and attributed to specific intracellular damage provoked by the local effect of MNPs on subcellular units.(Creixell, Bohórquez, Torres-Lugo & Rinaldi, 2011) (Villanueva et al., 2010) (Asin, Goya, Tres & Ibarra, 2013) (Hildebrandt et al., 2002),(Asin, Ibarra, Tres & Goya, 2012) However, the induced cell death observed in the present experiments could have been further promoted by the effects of the therapeutic drug loaded into the CSNPs. The application of a second MH treatment on A-172 cells induced further cellular damage so that cells looked smaller than cells subjected to 1 MH treatment and appeared as a round or oval mass. This effect was more evident for cells treated with 5-FU-CS-NPs and 5-FU-CS-MNP5.6. Interestingly, A-172 cells treated with CS-MNP5.6, showed cell regeneration after 2 MH treatments as evidenced by the formation of long filopodia.

The results corresponding to the cell viability of FBH and A-172 cells fixed 10 minutes after the application of 1 MH treatment are depicted in figure 7a. As can be observed, there is a significant reduction of the cell viability as a function of cell type being malignant human glioblastoma (A-172) more sensitive to the MH treatment than normal cells (FBH). In fact, FBH treated with all the samples under study presented cell viabilities higher than ~94 %, confirming that the MH treatment does not have an important effect on these cells. On the contrary, A-172 treated with CSNPs presented an important decrease in the cell viability with respect to the control for the three samples under study. For A-172 treated with 5-FU-CS-NPs, the decrease in cell viability is due to the antitumoral effect of 5-FU

Interestingly, similar cell viability values were achieved for A-172 cells incubated with 5-FU-CS-MNP5.6 and CS-MNP5.6. For sample CS-MNP5.6, the decrease of cell viability can be abscribed to the effect of magnetic hyperthermia. In the case of sample 5-FU-CS-MNP5.6, it is important to take into account that the % cumulative 5-FU release is significantly lower than the corresponding to 5-FU-CS-NPs as shown in figure 3. Therefore, the application of 1 MH treatment combined with a lower dose of 5-FU allows for a decrease in cell viability similar to the one found for samples incubated with 5-FU-CS-NPs thus proving the effective combination of magnetic hyperthermia and drug delivery.

In order to determine the ability of A-172 cells to regenerate after having been subjected to 1 MH treatment, the cell viability was compared for cells fixed 10 minutes and 4 hours after 1MH treatment. A-172 cells fixed 4 hours after the application of 1MH treatment (figure 7b) show an increase in cell viability with respect to A-172 cells fixed 10 minutes after the application of 1MH treatment (figure 7a) for all the samples under study which evidences cell regeneration. In addition, cell viability was compared for A-172 cells subjected to one and two MH treatments (figure 7b). A-172 cells incubated with CS-MNP5.6 show an increase of cell viability after the application of 2 MH treatments. This result could be attributed to the cell proliferation rate of A-172 cells in the presence of CS-MNP5.6 which overcomes the cellular death and it also suggest that some of the cells damaged during the 1 MH treatment appear as ‘healthy’ cells after few hours (4 hours). As expected, A-172 cells treated with sample 5-FU-CS-NPs, which did not contain magnetic nanoparticles, did not present a significant change in cell viability. In contrast, samples treated with 5-FU-CS-MNP5.6 presented a slight decrease in cell viability after 2 MH treatments compared to the cell viability found after 1 MH treatment. This result further confirms the combined effect of the 5-FU that

continues to be released during the period of the treatment, together with the application of magnetic hyperthermia. The results found demonstrate that cells treated with CS-MNP5.6 are able to regenerate after MH treatment and thus, a combination of chemotherapy and magnetic hyperthermia is needed to increase the efficacy of treatment.

Fluorescence images allows to obtain further information on cell death of FBH and A-172 cells after having been subjected to 1 and 2 MH treatments. As shown in figure 8, AO/PI staining allows recognizing easily dead cells (red fluorescence), lived cells (green fluorescence) and cells in the process of death (orange fluorescence). The red fluorescence highly increases for A-172 cell lines with respect to fibroblast which indicates a higher number of dead cells in this case.

Figure S6 in supplementary info shows representative photographs of A-172 cells incubated with 5-FU-CS-NPs, obtained after AO/PI staining and crystal violet staining after having been subjected to 1MH treatment. A vacuolization process (circles) can be observed which is characterized by the appearance of empty bags into the cytoplasm, indicating that cells are in process death. All these bags are enclosed within an intact plasma membrane, which is an important feature for apoptosis Also, typical nuclei separation and chromatin condensation related with apoptosis was observed (Elmore, 2007). AO/PI staining, for A-172 cell treated with CSNPs subjected to 2 MH treatments show significant evidence of cellular death and cells in process of death, recognized by the orange cells which are more visible in photographs corresponding to cells treated with 5-FU-CS-NPs and 5-FU-CS-MNP5.6.

4. Conclusions

We have succeeded in producing a responsive material based on ionotropic coupled chitosan nanoparticles loaded with 5-FU and magnetic iron oxide nanoparticles. The concurrency of a good encapsulation and loading efficiency of the CSNPs (within the 80-85% and 30-36% range, respectively) indicate the potential of these materials for therapeutic purposes. It was demonstrated that the drug delivery profile of 5-FU from CSNPs can be modulated as a function of the concentration of MNPs, so that a higher content leads to a lower 5-FU release from CSNPs at physiological pH. CSNPs were successfully internalized over normal cells (fibroblasts) and malignant human glioblastoma cells (A-172). A dose-dependent cytotoxic effect was found for both cell lines, with A-172 cells being more sensitive than fibroblasts to CSNPs loaded with 5-FU and iron oxide nanoparticles. Magnetic hyperthermia treatment was applied over fibroblast and malignant human glioblastoma cells (A-172) treated with CSNPs. After MH treatment, the cell viability for A-172 cells was on the range of 67-75% whereas for fibroblasts the cell viability was higher than ~94%. Therefore, A-172 cells were more sensitive to MH treatment than fibroblasts. Nevertheless, A-172 cells are able to regenerate when samples are observed 4 h after the application of a MH treatment. The application of a second MH treatment combined with 5-FU action leads to a higher efficacy of treatment. In view of the results obtained, CSNPs loaded with 5-FU and ferrofluid, can be considered as potential nanocarriers after the optimization of the preparation conditions for combined drug delivery and hyperthermia application, achieving a reduction of cell viability and inducing apoptosis after MH treatment.

ACKNOWLEDGEMENTS

The authors would like to express their appreciation to D. Gómez and P. Posadas for FESEM microscopy and AFM measurements and R. Ramirez for cell culture studies.

V. Zamora-Mora thanks CSIC for a JAE predoc fellowship and R. Hernández thanks MEC for a Ramon y Cajal contract. Financial support from the Spanish Ministerio de Economía y Competitividad (MINECO) (projects MAT 2011-24797, MAT2010-19326 and HelloKit INNPACTO) is also acknowledged.

5. References

Asin, L., Goya, G. F., Tres, A., & Ibarra, M. R. (2013). Induced cell toxicity originates dendritic cell death following magnetic hyperthermia treatment. *Cell Death and Disease, 4*, e596.

Asin, L., Ibarra, M. R., Tres, A., & Goya, G. F. (2012). Controlled cell death by magnetic hyperthermia: effects of exposure time, field amplitude, and nanoparticle concentration. *Pharm Res, 29*(5), 1319-1327.

C. Peniche, F.M. Goycoolea, & Argüelles-Monal, W. (2008). Chitin and Chitosan: Major Sources, Properties and Applications. In M.N. Belgacem & A. Gandini (Eds.). *Monomers, Polymers and Composites from Renewable Resources* (Vol. 1, pp. 517-542): Elsevier.

Creixell, M., Bohórquez, A. C., Torres-Lugo, M., & Rinaldi, C. (2011). EGFR-Targeted Magnetic Nanoparticle Heaters Kill Cancer Cells without a Perceptible Temperature Rise. *ACS Nano, 5*(9), 7124-7129.

Chen, J., Huang, L., Lai, H., Lu, C., Fang, M., Zhang, Q., & Luo, X. (2014). Methotrexate-Loaded PEGylated Chitosan Nanoparticles: Synthesis, Characterization, and in Vitro and in Vivo Antitumoral Activity. *Molecular Pharmaceutics, 11*(7), 2213-2223.

Dash, M., Chiellini, F., Ottenbrite, R. M., & Chiellini, E. (2011). Chitosan—A versatile semi-synthetic polymer in biomedical applications. *Progress in Polymer Science, 36*(8), 981-1014.

de la Fuente, M., Raviña, M., Paolicelli, P., Sanchez, A., Seijo, B., & Alonso, M. J. (2010). Chitosan-based nanostructures: A delivery platform for ocular therapeutics. *Advanced Drug Delivery Reviews, 62*(1), 100-117.

Deng, Z., Zhen, Z., Hu, X., Wu, S., Xu, Z., & Chu, P. K. (2011). Hollow chitosan–silica nanospheres as pH-sensitive targeted delivery carriers in breast cancer therapy. *Biomaterials, 32*(21), 4976-4986.

Donadel, K., Felisberto, M. D. V., Fávere, V. T., Rigoni, M., Batistela, N. J., & Laranjeira, M. C. M. (2008). Synthesis and characterization of the iron oxide magnetic particles coated with chitosan biopolymer. *Materials Science and Engineering: C, 28*(4), 509-514.

Elmore, S. (2007). Apoptosis: A Review of Programmed Cell Death. *Toxicologic Pathology, 35*(4), 495-516.

Fernandes, S. C., de Oliveira, I. R. W. Z., Fatibello-Filho, O., Spinelli, A., & Vieira, I. C. (2008). Biosensor based on laccase immobilized on microspheres of chitosan crosslinked with tripolyphosphate. *Sensors and Actuators B: Chemical, 133*(1), 202-207.

Fernández-Quiroz, D., González-Gómez, Á., Lizardi-Mendoza, J., Vázquez-Lasa, B., Goycoolea, F. M., San Román, J., & Argüelles-Monal, W. M. (2015). Effect of the molecular architecture on the thermosensitive properties of chitosan-g-poly(N-vinylcaprolactam). *Carbohydrate Polymers, 134*, 92-101.

Goya, G. F., Lima, E., Arelaro, A. D., Torres, T., Rechenberg, H. R., Rossi, L., Marquina, C., & Ibarra, M. R. (2008). Magnetic Hyperthermia With Fe3O4 Nanoparticles: The Influence of Particle Size on Energy Absorption. *IEEE TRANSACTIONS ON MAGNETICS, 44*(11), 4444-4447.

Guo, H., Chen, W., Sun, X., Liu, Y.-N., Li, J., & Wang, J. (2015). Theranostic magnetoliposomes coated by carboxymethyl dextran with controlled release by low-frequency alternating magnetic field. *Carbohydrate Polymers, 118*, 209-217.

Gupta, A. K., & Gupta, M. (2005). Cytotoxicity suppression and cellular uptake enhancement of surface modified magnetic nanoparticles. *Biomaterials, 26*(13), 1565-1573.

Gupta, A. K., & Gupta, M. (2005). Synthesis and surface engineering of iron oxide nanoparticles for biomedical applications. *Biomaterials, 26*(18), 3995-4021.

Hervault, A., & Thanh, N. n. T. K. (2014). Magnetic nanoparticle-based therapeutic agents for thermo-chemotherapy treatment of cancer. *Nanoscale, 6*(20), 11553-11573.

Hildebrandt, B., Wust, P., Ahlers, O., Dieing, A., Sreenivasa, G., Kerner, T., Felix, R., & Riess, H. (2002). The cellular and molecular basis of hyperthermia. *Critical Reviews in Oncology/Hematology, 43*(1), 33-56.

Huang, C., Neoh, K. G., Xu, L., Kang, E. T., & Chiong, E. (2012). Polymeric Nanoparticles with Encapsulated Superparamagnetic Iron Oxide and Conjugated Cisplatin for Potential Bladder Cancer Therapy. *Biomacromolecules, 13*(8), 2513-2520.

Jordan, A., Scholz, R., Wust, P., Fähling, H., & Roland, F. (1999). Magnetic fluid hyperthermia (MFH): Cancer treatment with AC magnetic field induced excitation of biocompatible superparamagnetic nanoparticles. *Journal of Magnetism and Magnetic Materials, 201*(1–3), 413-419.

Kumar, C. S. S. R., & Mohammad, F. (2011). Magnetic nanomaterials for hyperthermia-based therapy and controlled drug delivery. *Advanced Drug Delivery Reviews, 63*(9), 789-808.

Laurent, S., Dutz, S., Häfeli, U. O., & Mahmoudi, M. (2011). Magnetic fluid hyperthermia: Focus on superparamagnetic iron oxide nanoparticles. *Advances in Colloid and Interface Science, 166*(1–2), 8-23.

Lawrie, G., Keen, I., Drew, B., Chandler-Temple, A., Rintoul, L., Fredericks, P., & Grøndahl, L. (2007). Interactions between Alginate and Chitosan Biopolymers Characterized Using FTIR and XPS. *Biomacromolecules, 8*(8), 2533-2541.

Longley, D. B., Harkin, D. P., & Johnston, P. G. (2003). 5-Fluorouracil: mechanisms of action and clinical strategies. *Nature Reviews Cancer, 3*(5), 330-338.

Lozano, M. V., Torrecilla, D., Torres, D., Vidal, A., Domínguez, F., & Alonso, M. J. (2008). Highly Efficient System To Deliver Taxanes into Tumor Cells: Docetaxel-Loaded Chitosan Oligomer Colloidal Carriers. *Biomacromolecules, 9*(8), 2186-2193.

Mahdavinia, G. R., Etemadi, H., & Soleymani, F. (2015). Magnetic/pH-responsive beads based on caboxymethyl chitosan and κ-carrageenan and controlled drug release. *Carbohydrate Polymers, 128*, 112-121.

Mignani, S., Bryszewska, M., Klajnert-Maculewicz, B., Zablocka, M., & Majoral, J.-P. (2015). Advances in Combination Therapies Based on Nanoparticles for Efficacious Cancer Treatment: An Analytical Report. *Biomacromolecules, 16*(1), 1-27.

Muzzarelli, R. A. A., & Muzzarelli, C. (2005). Chitosan Chemistry: Relevance to the Biomedical Sciences. In T. Heinze (Ed.). *Polysaccharides I* (Vol. 186, pp. 151-209): Springer Berlin Heidelberg.

Papadimitriou, S., Bikiaris, D., Avgoustakis, K., Karavas, E., & Georgarakis, M. (2008). Chitosan nanoparticles loaded with dorzolamide and pramipexole. *Carbohydrate Polymers, 73*(1), 44-54.

Rescignano, N., Fortunati, E., Armentano, I., Hernandez, R., Mijangos, C., Pasquino, R., & Kenny, J. M. (2015). Use of alginate, chitosan and cellulose nanocrystals as emulsion stabilizers in the synthesis of biodegradable polymeric nanoparticles. *Journal of Colloid and Interface Science, 445*(0), 31-39.

Unsoy, G., Khodadust, R., Yalcin, S., Mutlu, P., & Gunduz, U. (2014). Synthesis of Doxorubicin loaded magnetic chitosan nanoparticles for pH responsive targeted drug delivery. *European Journal of Pharmaceutical Sciences, 62*, 243-250.

Vårum, K. M., Antohonsen, M. W., Grasdalen, H., & Smidsrød, O. (1991). Determination of the degree of N-acetylation and the distribution of N-acetyl groups in partially N-deacetylated chitins (chitosans) by high-field n.m.r. spectroscopy. *Carbohydrate Research, 211*(1), 17-23.

Villanueva, A., de la Presa, P., Alonso, J. M., Rueda, T., Martínez, A., Crespo, P., Morales, M. P., Gonzalez-Fernandez, M. A., Valdés, J., & Rivero, G. (2010). Hyperthermia HeLa Cell Treatment with Silica-Coated Manganese Oxide Nanoparticles. *The Journal of Physical Chemistry C, 114*(5), 1976-1981.

Wang, Z., Zeng, R., Tu, M., & Zhao, J. (2013). Synthesis, characterization of biomimetic phosphorylcholine-bound chitosan derivative and in vitro drug release of their nanoparticles. *Journal of Applied Polymer Science, 128*(1), 153-160.

Wei, W., Lv, P.-P., Chen, X.-M., Yue, Z.-G., Fu, Q., Liu, S.-Y., Yue, H., & Ma, G.-H. (2013). Codelivery of mTERT siRNA and paclitaxel by chitosan-based nanoparticles promoted synergistic tumor suppression. *Biomaterials, 34*(15), 3912-3923.

Yang, C.-H., Lin, Y.-S., Huang, K.-S., Huang, Y.-C., Wang, E.-C., Jhong, J.-Y., & Kuo, C.-Y. (2009). Microfluidic emulsification and sorting assisted preparation of monodisperse chitosan microparticles. *Lab on a Chip, 9*(1), 145-150.

Zamora-Mora, V., Fernández-Gutiérrez, M., Román, J. S., Goya, G., Hernández, R., & Mijangos, C. (2014). Magnetic core–shell chitosan nanoparticles: Rheological characterization and hyperthermia application. *Carbohydrate Polymers, 102*, 691-698.

Zhao, D.-L., Wang, X.-X., Zeng, X.-W., Xia, Q.-S., & Tang, J.-T. (2009). Preparation and inductive heating property of Fe3O4-chitosan composite nanoparticles in an AC magnetic field for localized hyperthermia. *Journal of Alloys and Compounds, 477*(1-2), 739-743.

Zhu, L., Ma, J., Jia, N., Zhao, Y., & Shen, H. (2009). Chitosan-coated magnetic nanoparticles as carriers of 5-Fluorouracil: Preparation, characterization and cytotoxicity studies. *Colloids and Surfaces B: Biointerfaces, 68*(1), 1-6.

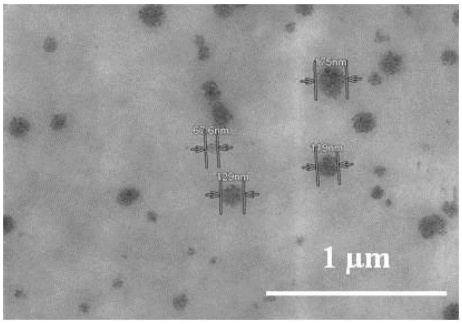

Figure 1. *Representative FESEM image corresponding to sample 5-FU-CS-MNP3.2*

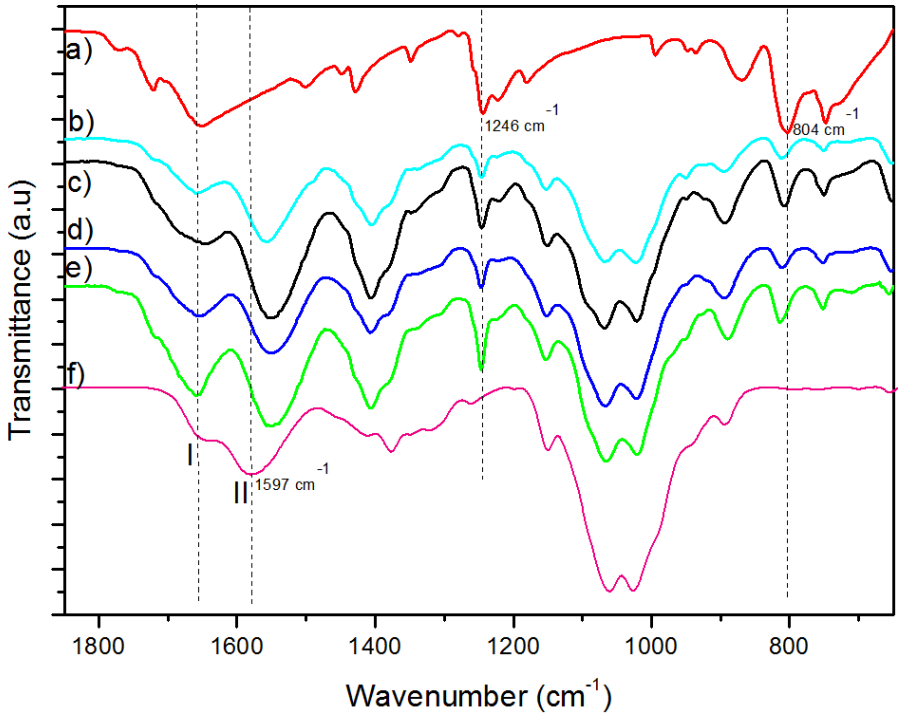

Figure 2. *ATR-FTIR spectra of a)5-FU, b)5-FU-CS-MNP5.6 c) 5-FU-CS-MNP3.2 d) 5-FU-CS-MNP1, e) 5-FU-CS-NPs and f) CS*

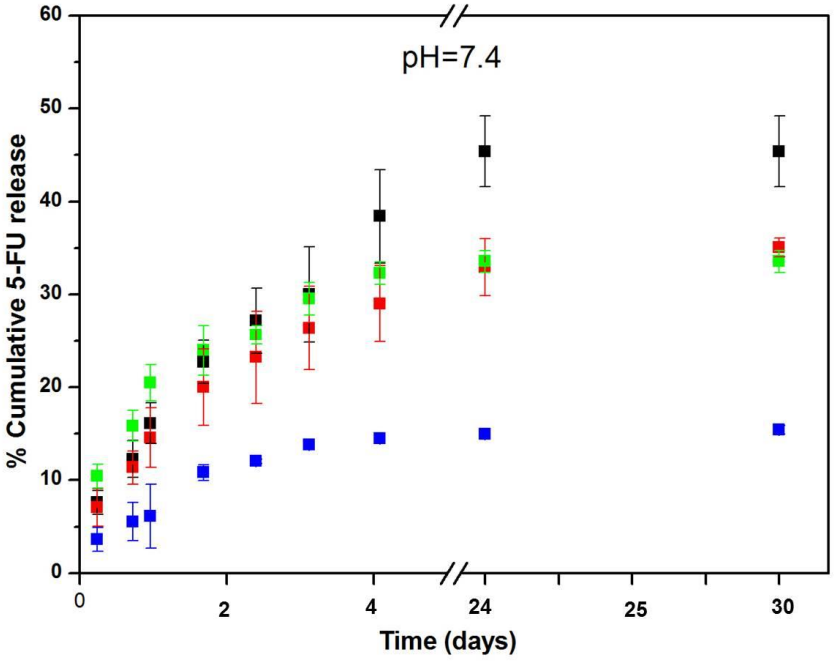

Figure 3. *In vitro release of 5-FU from CSNPs measured at pH=7.4,* (■) 5-FU-CS-NPs, (■) 5-FU-CS-MNP1, (■) 5-FU-CS-MNP3.2 and (■) 5-FU-CS-MNP5.6.

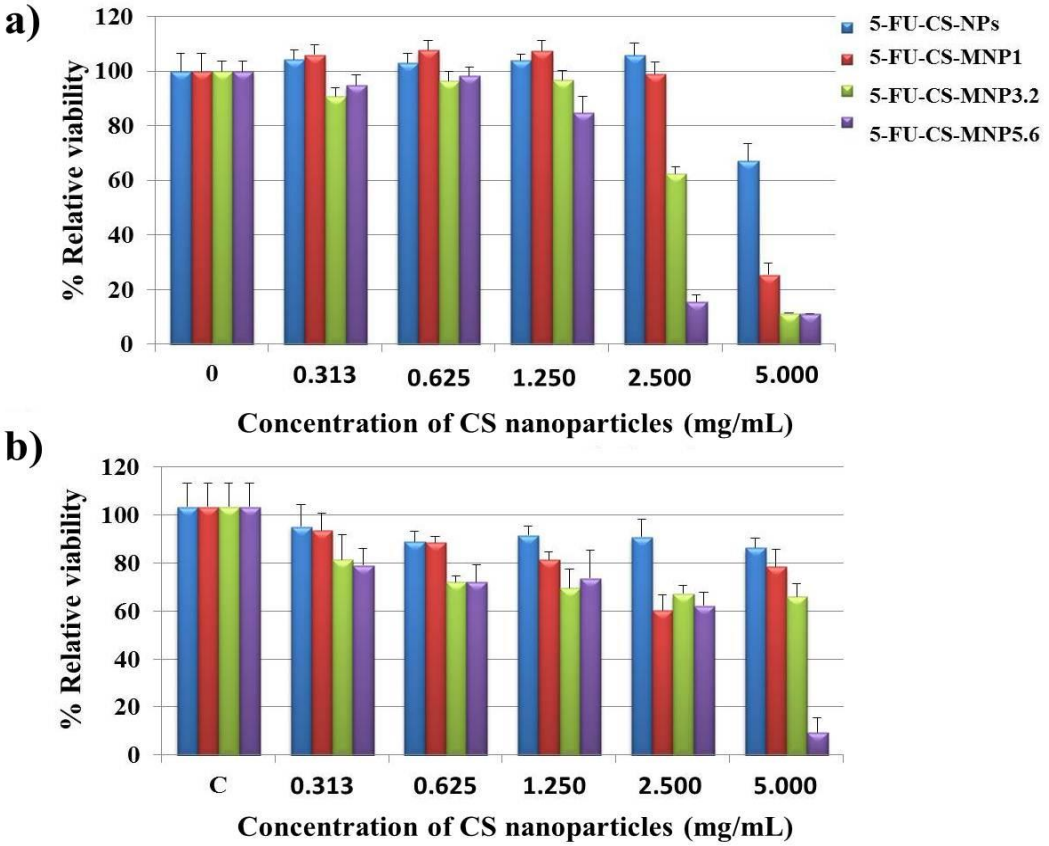

Figure 4. *Evaluation of cytotoxicity of CS nanoparticles under study on a) normal cells, FBH and b) cancer cells, A-172. % relative cell viability was measured using Alamar Blue assay. All the results are shown as mean n=4 ±S.D.*

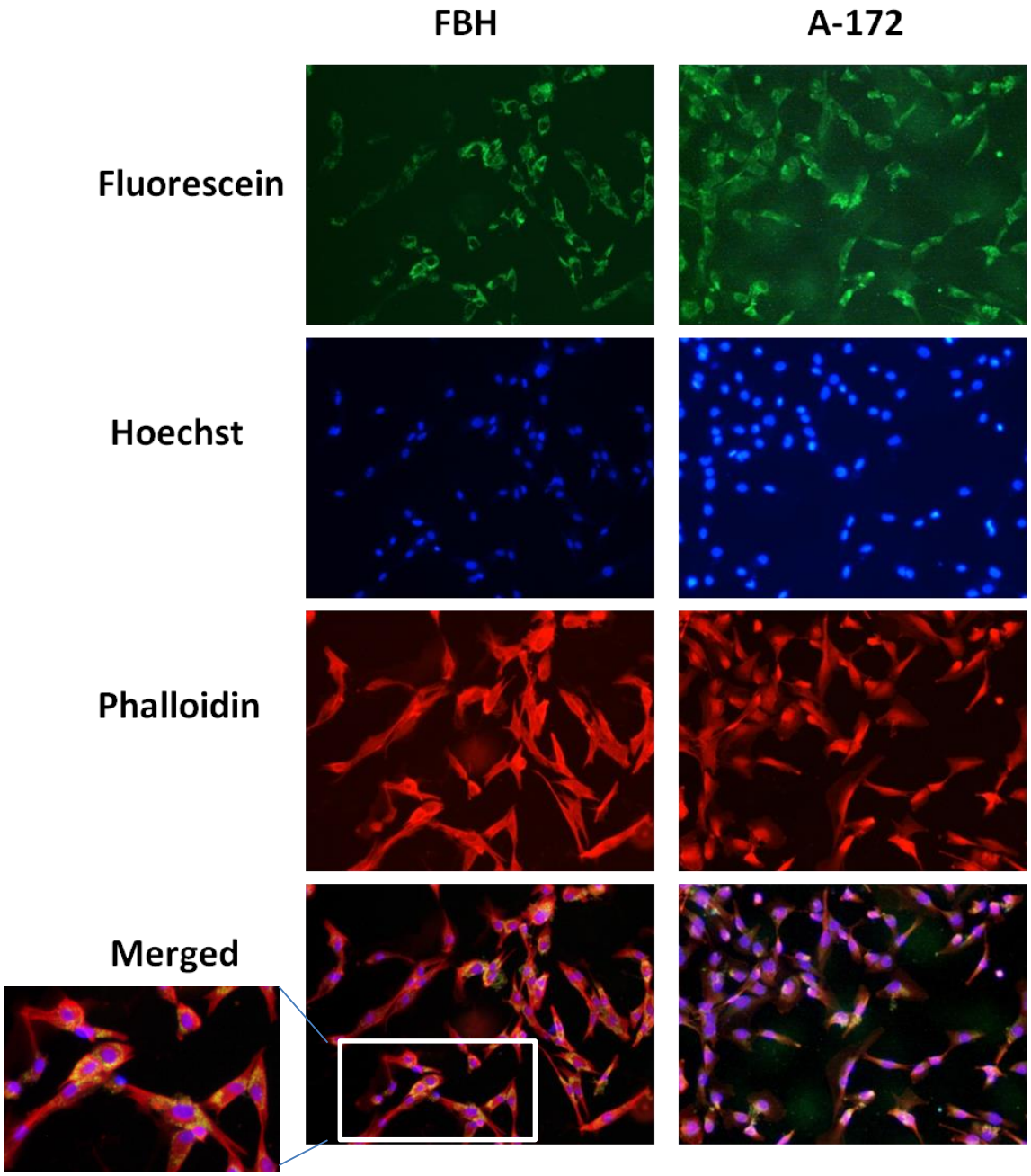

Figure 5. *Uptake studies for 5-FU-CS-MNP5.6 after 24 h of incubation, for normal cells, FBH and cancer cells, A-172. For easier visualization of 5-FU-CS-MNP5.6 inside the cells, a magnification of the merged image corresponding to FBH has been added as inset.*

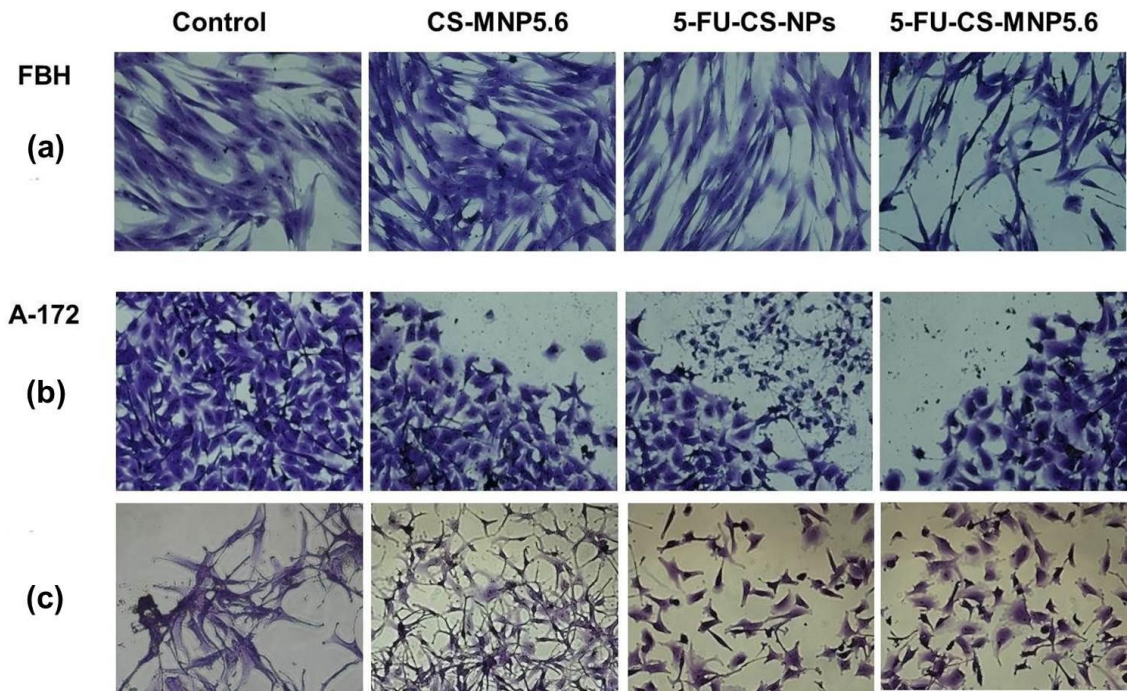

Figure 6. *Photographs (10x) of crystal violet staining for FBH subjected to a) 1 MH treatment and A-172 cells subjected to b) 1MH and c) 2 MH treatments.*

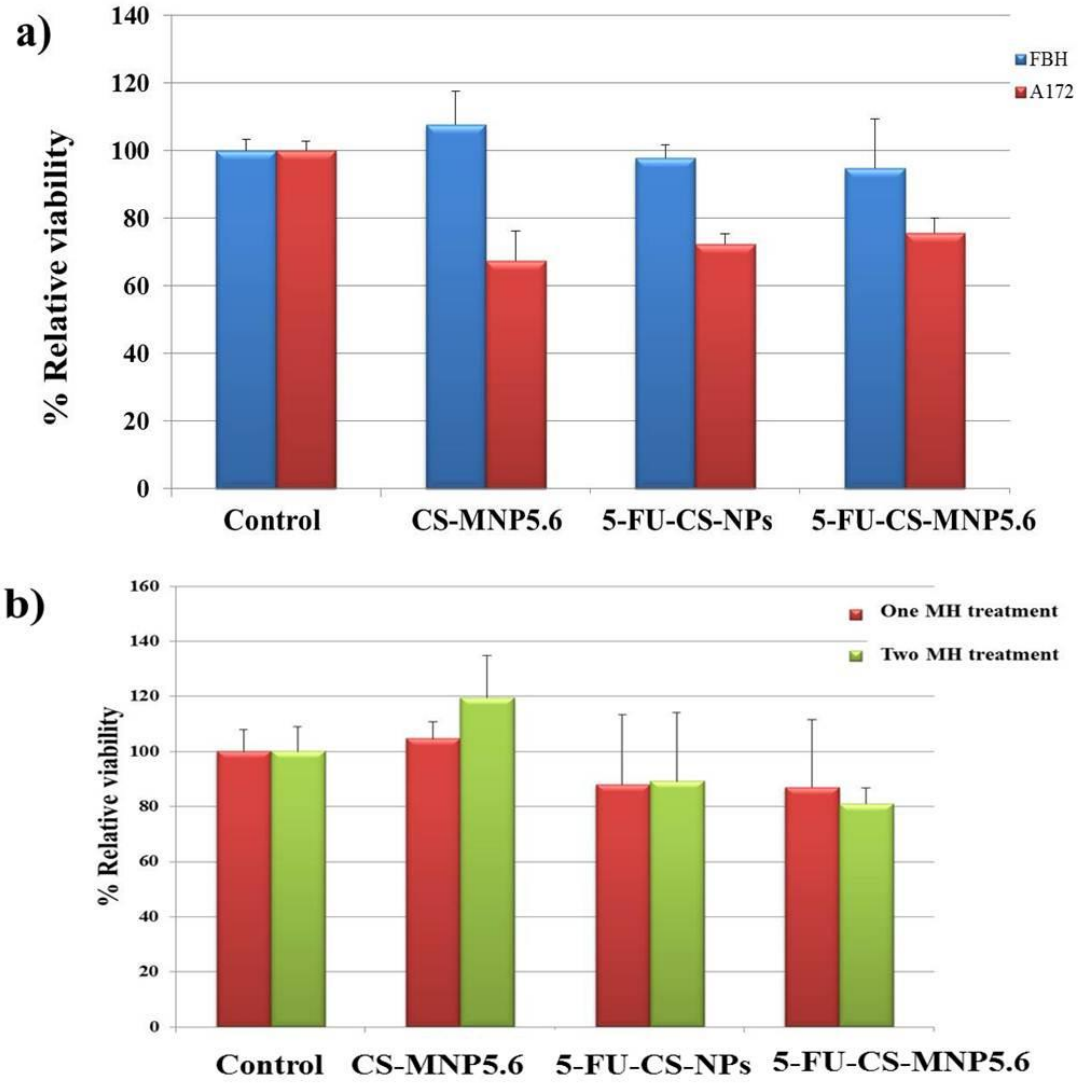

Figure 7. *% Relative cell viability obtained from crystal violet staining experiments for a) FBH and A-172 cells incubated with CS-MNP5.6, 5-FU-CS-NPs and 5-FU-CS-MNP5.6 fixed 10 minutes after 1MH treatment and b) A-172 cells fixed 4 hours after 1 MH treatment and 2 MH treatments.*

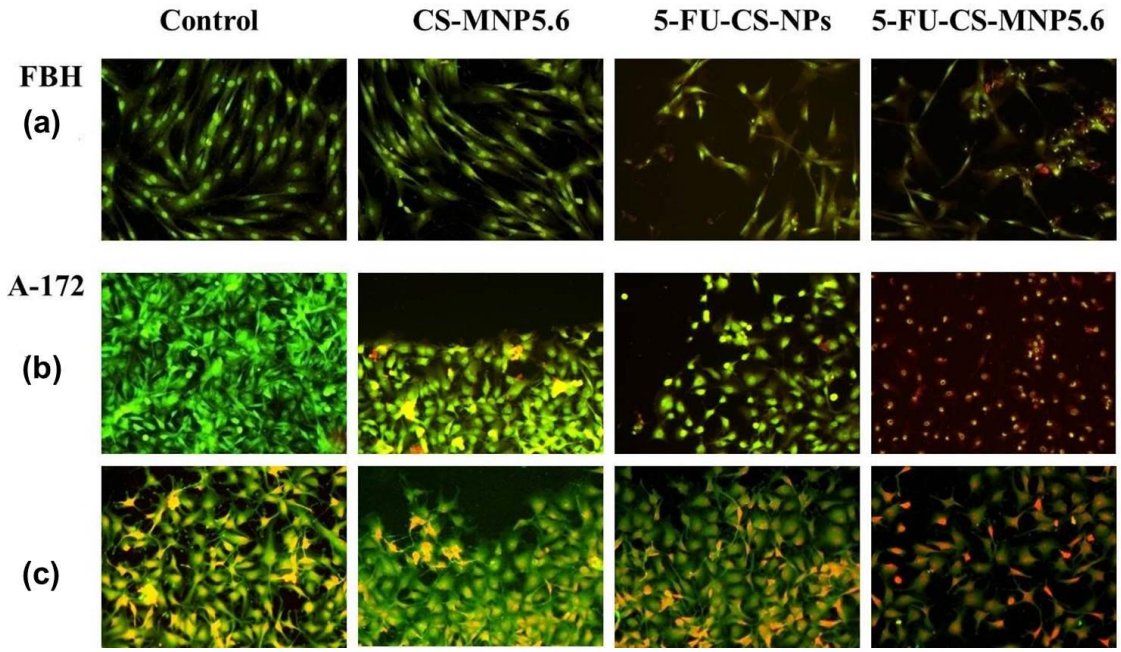

Figure 8. *Fluorescence images obtained after AO/PI staining for FBH subjected to a) 1 MH treatment and A-172 cells subjected to b) 1MH and c) 2 MH treatments.*

Table 1. Hydrodynamic diameter (nm) and ζ–potential (mV) of CSNPs

Sample	Hydrodynamic diameter (nm)	ζ–potential (mV)
5-FU-CS-NPs	183±2	+52.5±1.2
5-FU-CS-MNP1	191±6	+55.2±0.9
5-FU-CS-MNP3.2	215±7	+58.0±0.8
5-FU-CS-MNP5.6	255±9	+59.0±0.9